# Epipolar Geometry for Panoramic Cameras *

Tomáš Svoboda, Tomáš Pajdla and Václav Hlaváč

Center for Machine Perception
Czech Technical University, Faculty of Electrical Engineering
121 35 Prague 2, Karlovo náměstí 13, Czech Republic
http://cmp.felk.cvut.cz

**Abstract.** This paper presents fundamental theory and design of *central panoramic cameras*. Panoramic cameras combine a convex hyperbolic or parabolic mirror with a perspective camera to obtain a large field of view. We show how to design a panoramic camera with a tractable geometry and we propose a simple calibration method. We derive the image formation function for such a camera. The main contribution of the paper is the derivation of the epipolar geometry between a pair of panoramic cameras. We show that the mathematical model of a central panoramic camera can be decomposed into two central projections and therefore allows an epipolar geometry formulation. It is shown that epipolar curves are conics and their equations are derived. The theory is tested in experiments with real data.

*Keywords:* omnidirectional vision, epipolar geometry, panoramic cameras, hyperbolic mirror, stereo, catadioptric sensors.

## 1 Introduction

It is well known that egomotion estimation algorithms in some cases cannot well distinguish a small pure translation of the camera from a small rotation. An example is a translation parallel to the image plane and a rotation around an axis perpendicular to the direction of the translation [6]. The confusion becomes dominant when the depth variations in the scene are small or if the field of view is narrow.

The confusion can be removed if a camera with a large field of view is used [6]. Ideally, one would like to use a panoramic camera which has complete 360° field of view and sees in all directions. Such panoramic camera can, in principle, obtain correspondences from everywhere independently of the direction of egomotion. The uncertainty of the motion estimation will therefore also become independent of the motion direction. The above intuitive reasoning has been formalized by

* This research was supported by the Czech Ministry of Education grant VS96049, the internal grant of the Czech Technical University 3097472/335, the Grant Agency of the Czech Republic, grants 102/97/0480, 102/97/0855 and European Union grant Copernicus CP941068.

the result of Brodský et al. [3] who show that the motion estimation is almost never ambiguous for the spherical imaging surface.

This work was motivated by improving stability of egomotion estimation by enlarging field of view of the camera. However, the results concerning epipolar geometry are general and can be used also for looking for stereo correspondences in panoramic images or reconstruction of a scene. In the sequel, we introduce a mathematical model of central panoramic cameras and derive epipolar geometry between a pair of them.

### 1.1 Work related to panoramic stereo

Though other researchers have already realized that the use of panoramic cameras improves egomotion estimation, little attention has been given to developing the geometry of moving panoramic images as is the *epipolar geometry* [7] for perspective camera. The closest related works by others are by Benosman et al. [2], Yagi et al. [19,20], Southwell et al. [17], Chahl et al. [4], and most recently by Nene et al. [15] and [9]. Benosman et al. use two $1024 \times 1$ line cameras rotating around a vertical axis. They get two panoramic images but does not calculate epipolar geometry since the corresponding features lie trivially in the same column. The disadvantage is the complicated construction of the sensor. Yagi at al. [19] developed a panoramic camera with a conic mirror. They use it for the detection of an azimuth of vertical lines. An acoustics sensor with an optical one is integrated and the trajectory of a mobile robot is found. In [20] a hyperbolic mirror is used, however swiveling motion is detected by analyzing an optical flow and no epipolar geometry is presented. Southwell et al. [17] propose an idea of the stereo with one camera and concentric double lobed mirror but they do not present solid mathematical background. Chahl and Srinivasan [4] draw a method for range estimation using panoramic sensor with the conic mirror. The approach is based on range dependency of motion–induced deformation of the panoramic image. Most recently, Nene and Nayar [15] offer a stereo sensor built from one standard camera and two mirrors. They establish the epipolar geometry for limited case of pure rotation (translation in the case of using parabolic mirror and orthographic camera) of the mirror around the camera. Gluckman and Nayar [9] estimate ego-motion of the omnidirectional cameras by an optical flow algorithm.

A number of authors use panoramic cameras for fast visualization of a complete surroundings of the observer or as a source of images in order to construct a scene representation for virtual reality [5,8,10,13,14].

## 2 Design of a panoramic camera

Several different designs of panoramic camera emerged recently. We do not consider panoramic vision systems with moving parts since they are not applicable for real time imaging due to considerable time needed to capture a panoramic image. Fleck [8] uses wide–angle lenses to capture a panoramic image covering

a hemisphere. However, such lenses are large and expensive [5]. A panoramic camera covering almost a whole imaging sphere can be obtained by combining a classical perspective (pinhole) camera with a convex mirror. Yagi uses a conic–shaped mirror [19] and hyperbolic mirror [20]. Hamit [10] describes various approaches to obtain panoramic images using different types of mirrors. Nayar presents [14, 10] several prototypes of panoramic cameras using a parabolic mirror in combination with orthographic cameras. Chahl and Srinivasan [5] study reflective surfaces preserving a linear relationship between the angle of incidence of light on the surface and the angle of reflection onto the imaging device. Most recently, independently of this work, Baker and Nayar [1] describe the class of convex mirrors preserving the single effective viewpoint.

The cameras based on convex mirrors offer large field of view (approx. $360° \times 150°$), instant image acquisition at video rate, compact design, cheap (US$220 for our hyperbolic mirror) production, and the freedom to choose the shape of the mirror in order to yield a nice mathematical model of the camera.

### 2.1 Shape of the mirror

A panoramic camera with a mirror, see Figure 1, consists of a perspective camera looking into a convex mirror. The ray $p_1$ proceeding from (or incoming into) the camera is reflected by the mirror as a ray $p_1'$. Each ray $p$ has to pass through the camera center of projection $C$. Reflected rays $p'$ can but need not intersect at the same point. Figure 1(a) shows a panoramic camera with a spherical mirror in which case the reflected rays do not intersect at the same point. Figure 1(b) shows the upper part of hyperboloid of two sheets, further called hyperbolic mirror, where all the reflected rays intersect at the focal point of the mirror $F'$. The camera center of projection $C$ coincides with the second focal point of the mirror, $F$. Figure 1(c) shows the parabolic mirror. Reflected rays $p_1', p_2'$ intersect in the focal point $F'$ of the mirror and the second mirror focus $F$ is at infinity thus the *orthographic* projection has to be used.

We further focus on the case when all reflected rays intersect at a single point. *This is an important property which is a necessary condition for the existence of epipolar geometry inherent to the moving sensor and independent of the scene structure.* Panoramic cameras with this property shall be called *central panoramic cameras.* In this case the model of the panoramic camera can be decomposed into a central projection from space onto a curved surface of the mirror and a central projection from the surface of the mirror into the image plane.

### 2.2 Model of a panoramic camera with a hyperbolic mirror

Figure 2 shows the composition of a perspective camera with a hyperbolic mirror so that the camera projection center $C$ coincides with the focal point of the mirror $F$. The perspective camera can be modeled by an *internal camera calibration matrix* $K$ which relates 3D coordinates $X = [x, y, z]^T$ into retinal coordinates $\mathbf{q} = [q_u, q_v, 1]^T$.

$$\mathbf{q} = \frac{1}{z} K X, \tag{1}$$

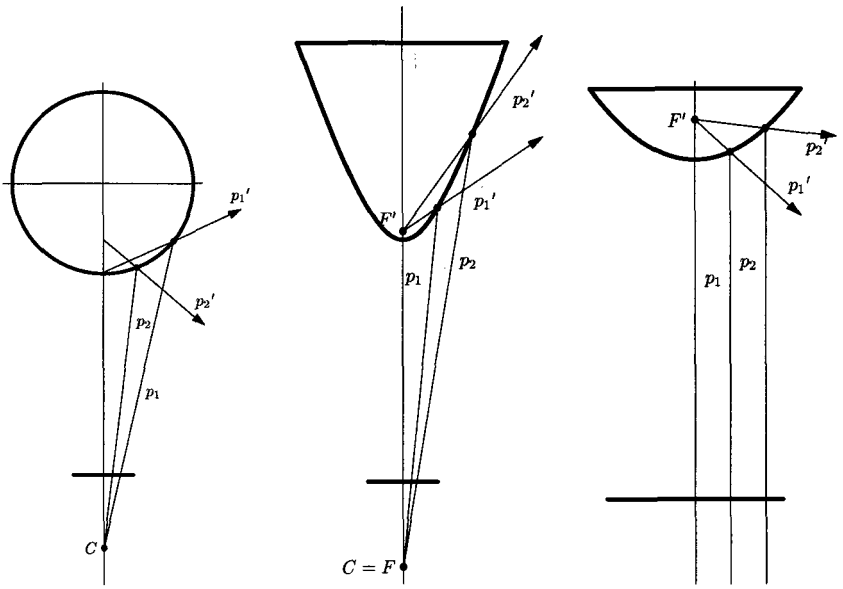


(a) Spherical mirror and a perspective camera. The reflected optical rays do not intersect in a unique point and the sensor suffers from spherical aberration.

(b) Hyperbolic mirror and a perspective camera. The reflected optical rays intersect in the focus of the hyperboloid.

(c) Parabolic mirror and a perspective camera. The reflected optical rays intersect in the focus of the paraboloid when orthographic projection is assumed.

**Fig. 1.** Three combinations lens–mirror.

See [7] for more information about camera calibration.

In the "mirror coordinate system", which is centered at the focal point $F'$, a hyperbolic mirror is defined by the equation

$$\frac{(z + \sqrt{a^2 + b^2})^2}{a^2} - \frac{x^2 + y^2}{b^2} = 1, \tag{2}$$

where $a$, $b$ are parameters of the mirror. The image formation can be expressed as a composition of the coordinate transformations and projections. We want to find the relationship between a point $X$ in the world coordinates and the camera point $\mathbf{q}$ in the retinal coordinate system. The derivation of the image formation is omitted here due to lack of space, details can be found in [18]. Complete model

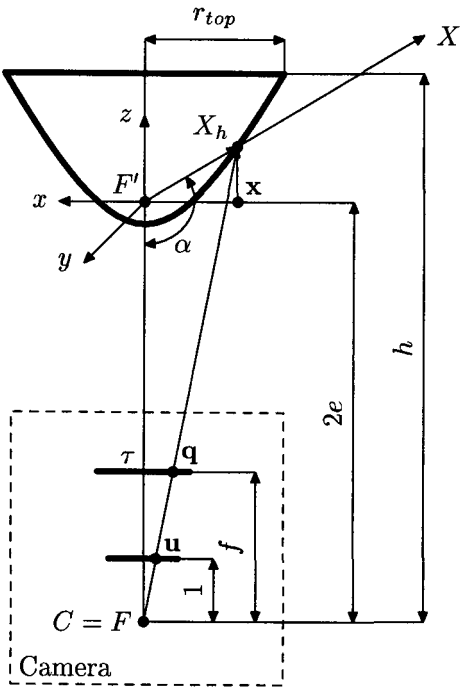


**Fig. 2.** The geometry of the mirror and the camera.

can be written concisely as

$$\mathbf{q} \simeq K R_C \Big( \mathcal{F}^-(R_M(X - \mathbf{t}_M)) R_M(X - \mathbf{t}_M) - \mathbf{t}_C \Big), \tag{3}$$

where $\simeq$ denotes equality up to nonzero scale. $R_C, \mathbf{t}_C$ express the rotation and translation between the mirror coordinate system and the camera coordinate system. $R_M, \mathbf{t}_M$ denote the transformation between the world and the mirror coordinate frames. $\mathcal{F}^-$ is the following nonlinear function of a 3D vector $\mathbf{v} = [v_1, v_2, v_3]^T$, which is in this case equal to $R_M(X - \mathbf{t}_M)$

$$\mathcal{F}^{\pm}(\mathbf{v}) = \frac{b^2(\pm e v_3 + a||\mathbf{v}||)}{b^2 v_3^2 - a^2 v_1^2 - a^2 v_2^2}, \text{ where } e = \sqrt{a^2 + b^2}. \tag{4}$$

Mapping (3) contains 6 external calibration parameters (3 for $\mathbf{t}_M$ and 3 for $R_M$) and 9 internal parameters ($a, b$ for the mirror, 2 for the rotation $R_C$, and 5 for $K$) [18]. The translation vector $\mathbf{t}_C = [0, 0, -2e]^T$ is indispensable, since the projection center of the camera has to coincide with the second focus of the hyperboloid.

In order to establish the equations for the epipolar geometry, it is necessary to find the coordinates of the point on the mirror $X_h$, see Figure 2, for each image point $\mathbf{q}$. The formula for computing $X_h$ from pixel coordinates $\mathbf{q}$ reads as

$$X_h = \mathcal{F}^+(R_C^T K^{-1} \mathbf{q}) R_C^T K^{-1} \mathbf{q} + \mathbf{t}_C, \tag{5}$$

where $\mathcal{F}^+(\mathbf{v})$ is given by equation (4).

# 3 Epipolar geometry of central panoramic cameras

## 3.1 Epipolar geometry for perspective cameras

Epipolar geometry of two perspective cameras [7], see Figure 3, assigns to each point $\mathbf{q}_1$ in one image an epipolar line $\mathbf{l}_2$ in the second image. All epipolar lines in each image intersect in the epipoles $\mathbf{e}_1$ and $\mathbf{e}_2$. Coordinates of an epipolar line

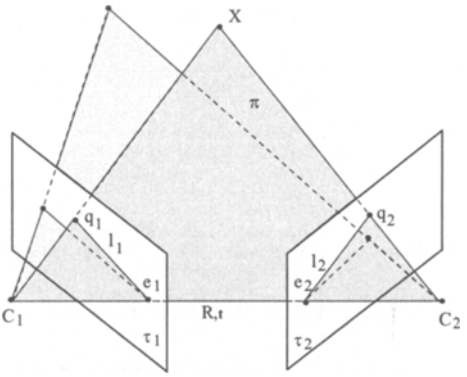


**Fig. 3.** The epipolar geometry of two perspective cameras.

can be defined as

$$\mathbf{l}_1 = \mathbf{q}_1 \wedge \mathbf{e}_1, \tag{6}$$

where the symbol $\wedge$ denotes a crossproduct. The equation (6) can be rewritten in a matrix form as

$$\mathbf{l}_1 = B(\mathbf{e}_1)\mathbf{q}_1. \tag{7}$$

The vector $\mathbf{l}_1$ is perpendicular to the line joining points $\mathbf{e}_1$ and $\mathbf{q}_1$ and points on this line satisfy $\mathbf{l}_1\mathbf{q} = 0$. Since the epipolar lines $\mathbf{l}_1$ and $\mathbf{l}_2$ are coplanar, the transformation between them is a collineation, defined by a $3 \times 3$ matrix A.

$$\mathbf{l}_2 = A\mathbf{l}_1. \tag{8}$$

By combining equations (8) and (7) together, we get

$$\mathbf{l}_2 = AB(\mathbf{e}_1)\mathbf{q}_1 = Q\mathbf{q}_1, \tag{9}$$

where $Q$ denotes the *fundamental matrix* [7]. Multiplying equation (9) by the $\mathbf{q}_2^T$ from the right side leaves us with

$$\mathbf{q}_2^T Q\mathbf{q}_1 = 0, \tag{10}$$

This equation says that the vector $\mathbf{t}$ connecting the centers of the cameras $C_1$ and $C_2$ is coplanar with the corresponding vectors $\mathbf{q}_1$ and $\mathbf{q}_2$.

### 3.2 Epipolar geometry for panoramic cameras

Let us define the translation $\mathbf{t}$ and the rotation $R$ between sensors as the translation and the rotation between local coordinate systems centered at mirror foci $F_1'$ and $F_2'$ , see Figure 4. Let points on the mirrors related to the a single 3D point be denoted $X_{h1}$ resp. $X_{h2}$, see Figure 4. The coplanarity of vectors $X_{h1}$, $X_{h2}$, and $\mathbf{t}$ can be written as

$$X_{h2} R(\mathbf{t} \wedge X_{h1}) = 0. \tag{11}$$

Introducing an antisymmetric matrix $S$

$$S = \begin{bmatrix} 0 & -t_z & t_y \\ t_z & 0 & -t_x \\ -t_y & t_x & 0 \end{bmatrix}, \tag{12}$$

we can rewrite the coplanarity constraint (11) in the matrix form as

$$X_{h2}^T E X_{h1} = 0, \text{ where } E = RS \tag{13}$$

stands for the *essential matrix*. The essential matrix $E$ can be used here instead of the fundamental matrix since vectors $X_{hi}$ are metric entities. Vectors $X_{h1}$, $X_{h2}$, and $\mathbf{t}$ form the *epipolar plane* $\pi$. This plane intersects the mirrors in space conics. These conics are then projected onto another conics in the image planes by a central (perspective) projection. A conic is uniquely assigned in the second image to a point $\mathbf{q}_1$ in the first image

$$\mathbf{q}_2^T A_2(E, \mathbf{q}_1)\ \mathbf{q}_2 = 0. \tag{14}$$

In general case, the matrix $A_2(E, \mathbf{q}_1)$ is a nonlinear function of the essential matrix $E$, point $\mathbf{q}_1$, and the calibration parameters of the panoramic cameras and the mirrors.

The shape of the conic, i.e. whether they are lines, ellipses, parabolas or hyperbolas, depends on the shape of mirrors, on motion of the cameras as well as on which pair of corresponding points in the images is considered. It holds that there is at least one line among all epipolar conics. It is the line which corresponds to the epipolar plane passing through the axis of the mirror. The corresponding epipolar curves are both lines iff the motion is a translation, i.e. the axes of the mirrors remain parallel. Moreover, if the translation is along the axis of the mirror, all epipolar curves become lines. It is clear that epipolar curves form a one-parameter family of conics which is parameterized by the angle of rotation of the epipolar planes around the vector $\mathbf{t}$.

All epipolar conics pass through two points which are the images of the intersection of mirrors with the line $F_1'F_2'$. Therefore, there are usually two epipoles, denoted $e_1$ and $e_1'$ resp. $e_2$ and $e_2'$ in Figure 4. The epipoles can degenerate into one double epipole if the camera is translated along the rotation axis of the rotation of the mirror.

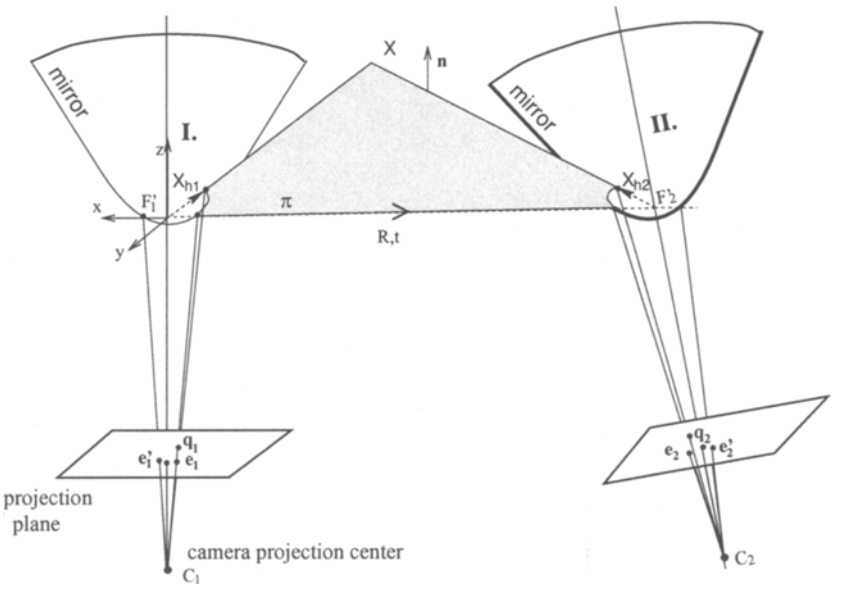


**Fig. 4.** The epipolar geometry of two panoramic cameras with hyperbolic mirrors.

### 3.3 Formula of epipolar conics

We look for the $A_2(E, \mathbf{q}_1)$ from equation (14). Let us find the equation of an orthographic projection of the space conic given by the intersection of the epipolar plane with the mirror to $xy$ plane of the mirror coordinate system, see Figure 4.

$$\mathbf{x}_2^T A_{\mathbf{x}_2} \mathbf{x}_2 = 0, \tag{15}$$

where

$$\mathbf{x}_2 = [x, y, 1]^T \text{ and } X_{h2} = [x, y, z]^T. \tag{16}$$

The focus of the first mirror $F_1'$, vectors $X_{h1}$ and $\mathbf{t}$ define the epipolar plane $\pi$. This plane intersects the second mirror in a planar conic. The normal vector of the plane $\pi$ expressed in the coordinate system of the first mirror is

$$\mathbf{n_1} = \mathbf{t} \wedge X_{h1}, \tag{17}$$

Normal vector $\mathbf{n}_1$ can be expressed in the coordinate system of the second mirror by using $E$, equation (13), as

$$\mathbf{n_2} = R\mathbf{n}_1 = R(\mathbf{t} \wedge X_{h1}) = RSX_{h1} = EX_{h1}. \tag{18}$$

Writing $\mathbf{n}_2 = [p, q, s]^T$, the equation of the plane $\pi$ can be written in the second coordinate system as

$$px + qy + sz = 0. \tag{19}$$

We can express $z$ as a function of $x, y$ from the equation (19) and substitute it into the equation (2) yielding us a polynomial in $x, y$

$$(p^2b^2 - s^2a^2)x^2 + 2pqb^2xy + (q^2b^2 - s^2a^2)y^2 - 2spb^2ex - 2sqb^2ey - s^2b^4 = 0, \quad (20)$$

which is actually the quadratic form of the conic (15). Parameters $a, b$ in equation (20) are related to the second mirror, since the epipolar plane, defined by the first mirror, intersects the second mirror. Consequently the matrix $A_{\mathbf{x}_2}$ from (15) has the form

$$A_{\mathbf{x}_2} = \begin{bmatrix} p^2b^2 - s^2a^2 & pqb^2 & -pseb^2 \\ pqb^2 & q^2b^2 - s^2a^2 & -qseb^2 \\ -pseb^2 & -qseb^2 & s^2b^4 \end{bmatrix}. \quad (21)$$

Let $s \neq 0$, i.e. the epipolar plane does not contain the axis of the mirror. Corresponding point in the second mirror $X_{h2}$ lies on the epipolar plane $\pi$. Substituting $x, y$ coordinates of $\mathbf{x}_2$ into equation (19), the coordinates of the point $X_{h2}$ can be expressed as a linear function of $\mathbf{x}_2$

$$X_{h2} = \begin{bmatrix} x \\ y \\ \frac{-px-qy}{s} \end{bmatrix} = \begin{bmatrix} 1 & 0 & 0 \\ 0 & 1 & 0 \\ -\frac{p}{s} & -\frac{q}{s} & 0 \end{bmatrix} \mathbf{x}_2. \quad (22)$$

It follows then from equations (5) and (22) that[1]

$$\mathcal{F}^+(R_C^T K^{-1}\mathbf{q}_2) R_C^T K^{-1}\mathbf{q}_2 = \left(X_{h2} + \begin{bmatrix} 0 \\ 0 \\ 2e \end{bmatrix}\right) = \begin{bmatrix} 1 & 0 & 0 \\ 0 & 1 & 0 \\ -\frac{p}{s} & -\frac{q}{s} & 2e \end{bmatrix} \mathbf{x}_2. \quad (23)$$

Since $\mathcal{F}^+(R_C^T K^{-1}\mathbf{q}_2) \neq 0$ for $s \neq 0$ we can write

$$\mathbf{x}_2 \simeq N R_C^T K^{-1}\mathbf{q}_2, \text{ where } N = \begin{bmatrix} 1 & 0 & 0 \\ 0 & 1 & 0 \\ \frac{p}{2se} & \frac{q}{2se} & \frac{1}{2e} \end{bmatrix}. \quad (24)$$

$\mathbf{x}_2$ can be then substituted into equation (15) yielding the desired equation of the epipolar conic in the image plane

$$\mathbf{q}_2^T K^{-T} R_C N^T A_{\mathbf{x}_2} N R_C^T K^{-1}\mathbf{q}_2 = 0, \quad (25)$$

leaving us with $A_2 = K^{-T} R_C B_2 R_C^T K^{-1}$, where

$$B_2 = N^T A_{\mathbf{x}_2} N = \begin{bmatrix} -4s^2a^2e^2 + p^2b^4 & pqb^4 & psb^2(-2e^2 + b^2) \\ pqb^4 & -4s^2a^2e^2 + q^2b^4 & qsb^2(-2e^2 + b^2) \\ psb^2(-2e^2 + b^2) & qsb^2(-2e^2 + b^2) & s^2b^4 \end{bmatrix} \quad (26)$$

[1] In (5), we use $\mathbf{t}_C = [0, 0, -2e]^T$ since the center of the camera has to coincide with the second focal point of the mirror.

is a nonlinear function of $a$, $b$, and

$$[p, q, s]^T = E\left(\mathcal{F}^+(R_C^T K^{-1}\mathbf{q}_1) R_C^T K^{-1}\mathbf{q}_1 - [0, 0, 2e]^T\right). \quad (27)$$

$\mathcal{F}^+(R_C^T K^{-1}\mathbf{q}_1)$ is defined by equation (4). Though we have assumed that $s \neq 0$ in the above development, equation (25) holds even for $s = 0$ as it can be verified by repeating the development for $X_{h2} = [x, y, 0]^T$ instead of equation (22) and comparing with the substitution of $s = 0$ into the equation (25).

Equation (25) defines the curve on which the projected corresponding point has to lie and it is indeed an equation of a conic as alleged by equation (14).

### 3.4 Using the epipolar geometry

The epipolar geometry presented above can be exploited similarly as in the case of standard perspective cameras. Once the epipolar geometry between two panoramic images is established, the search for correspondences is nicely reduced to 1 degree of freedom problem. At least 8 correspondences are needed to solve essential matrix linearly (13), using method [12], for instance. If the essential matrix $E$ is known we can compute epipolar conic for each point of interest in the first image, on which the corresponding point has to lie in the second image. We can then employ an iterative algorithm to establish epipolar geometry and to find correspondences more robustly [21].

Let the essential matrix $E$ be robustly estimated, from equation (13). Recall that $E = RS$, where $R$ is a rotation matrix and matrix $S$ is formed by elements of the translation vector $\mathbf{t}$, see equation (12). The *motion parameters* $R$ and $\mathbf{t}$ can be recovered using the approach described in [11], for instance.

## 4 Experiments

Our panoramic (omnidirectional) camera is intended for use in our mobile robot. The camera is below the mirror. We designed the mirror that the high vertical angle of view with the values $a = 28.1851$ mm and $b = 9.3950$ mm was obtained, see [18]. The mirror was manufactured by ASTRO—Telescope, Přerov, Czech Republic.

**Assembly.** We calibrated the standard CCD camera off–line, using the method and the equipment from [16]. The focal length $f$ of the camera used is 8.5 mm and the camera resolution is 768 × 512 pixels. To position camera correctly, we projected the calibration circle and the calibration axes into the image and moved the mirror until the axis of the mirror fits the calibration axes and the mirror rim fits the calibration circle.

**Sequence.** We captured a sequence by moving the panoramic sensor through our laboratory. The area, in which the sensor moved, was approximately 6 × 6

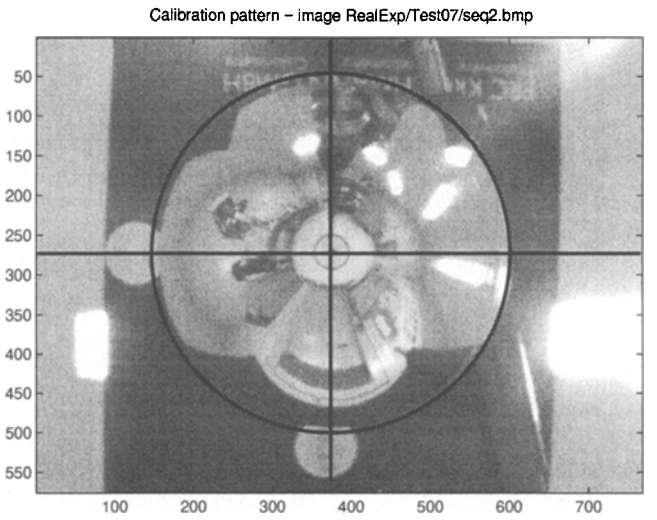


**Fig. 5.** Assembly of the sensor. The mirror fits the projected calibration circle and the calibration cross.

meters. The camera is below the mirror and the sensor is moving near the floor. Two consecutive images are shown in Fig 6. The points of interest were selected manually. There is no rotation between the two positions, because it is difficult to rotate the real sensor in a controlled way. The translation between two positions is $\mathbf{t} = [60, 60, 0]$ cm.

Although we used a very simple method to adjust the camera and mirror so that $C = F$, and no correction to radial distortion of the lens was used, the results are acceptable, see Figure 7. The epipolar conics pass very close to their corresponding point, see Figure 7. The inaccuracy is about two pixels, what is sufficient to find correspondences along conics. Three conics intersect in the epipole exactly.

## 5 Summary

This paper presented the fundamental theory and design of the central panoramic cameras. We presented an approach to design of a useful panoramic camera and we proposed a simple adjustment method. We defined the image formation function for such a camera. *Our main contribution is the derivation of epipolar geometry for panoramic cameras.*

Even when a simple adjustment method of the sensor was used, results corroborate our theory. The epipolar conics lie close to the corresponding points. The errors were about two pixels.

There are severeal questions which remain beyond the scope of this paper. It is a question how will the lower resolution affect the quality of motion estimation. Special care needs to be taken to finding an automatic calibration and

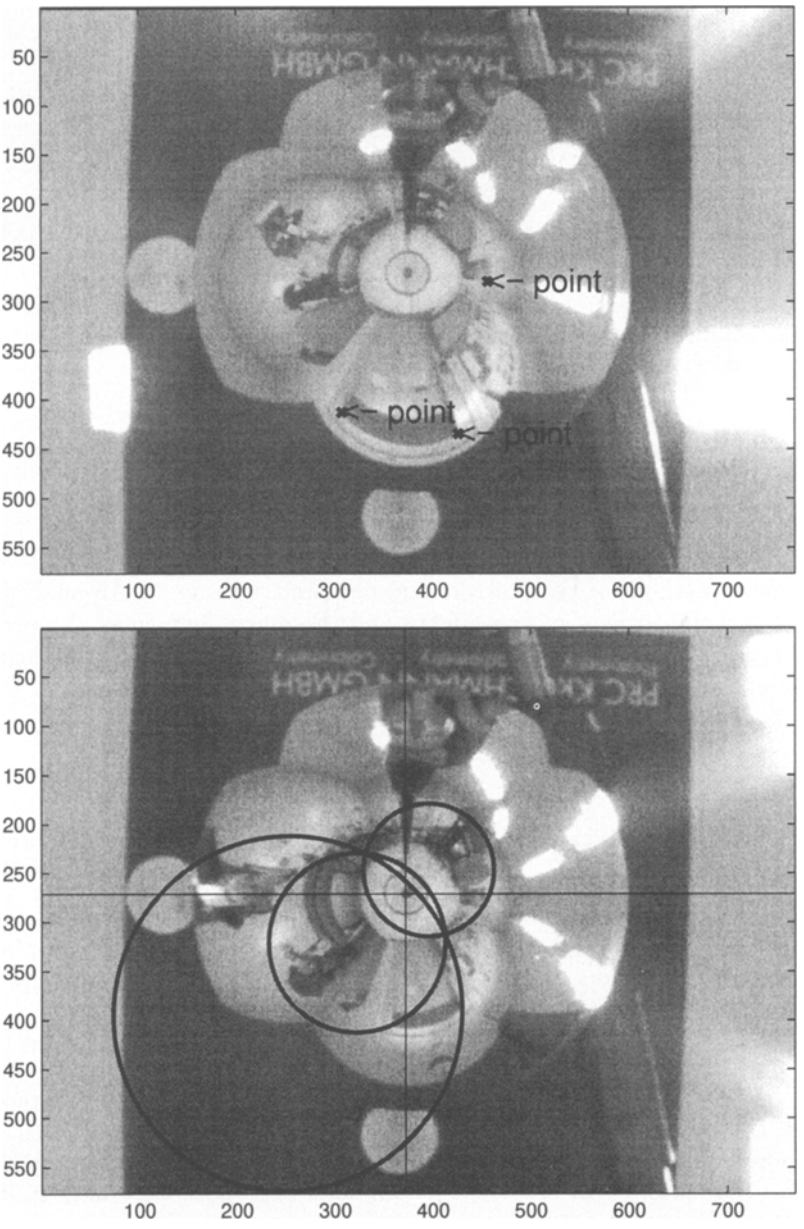


**Fig. 6.** Two panoramic images. Translation in $x$ and $y$ axis. Points of interest are marked in the upper image. Related epipolar conics are drawn in the bottom image. The conics pass through the corresponding points and intersect in two epipoles.

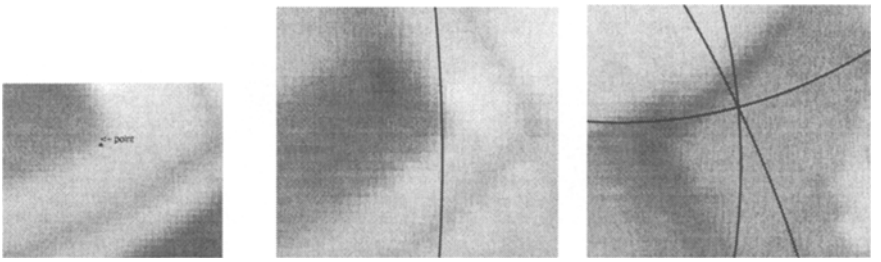

(a) Point in the corner of the jamb of the laboratory door.

(b) Related epipolar conics passes close to the corner in the second image. The error is less than 2 pixels.

(c) The epipolar conics intersect in the epipole.

**Fig. 7.** Details from the real images, shown in Figure 6.

adjustment method for real mirrors and perspective cameras. An analysis how an incorrect adjustment of the camera and the mirror influences the precision of the epipolar geometry need to be further worked out. More experiment with the stability of ego-motion computation are needed.

## References


1. Simon Baker and Shree K. Nayar. A theory of catadioptric image formation. *Submitted to IJCV*, 1997. Also appears in ICCV98, and exists as TR CUCS-015-97, and it was presented in Darpa IUW 1997.
2. R. Benosman, T. Maiere, and J. Devars. Multidirectional stereovision sensor, calibration and scenes reconstruction. In *International Conference on Pattern Recognition 1996, Vienna, Austria*, pages 161–165. IEEE Computer Society Press, September 1996.
3. T. Brodský, C. Fernmüller, and Y. Aloimonos. Directions of motion fields are hardly ever ambiguous. In Buxton. B. and R. Cipola, editors, *4th European Conference on Computer Vision, Cambridge UK*, volume 2, pages 119–128, 1996.
4. J.S. Chahl and M.V. Srinivasan. Range estimation with a panoramic visual sensor. *Journal of the Optical Society of America*, 14(9):2144–2151, September 1997.
5. J.S. Chahl and M.V. Srinivasan. Reflective surfaces for panoramic imaging. *Applied Optics*, 36(31):8275–8285, November 1997.
6. K. Daniilidis and H.-H. Nagel. The coupling of rotation and translation in motion estimation of planar surfaces. In *IEEE Conf. on Computer Vision and Pattern Recognition*, pages 188–193, New York, NY, June 1993.
7. Olivier Faugeras. *3-D Computer Vision, A Geometric Viewpoint*. MIT Press, 1993.
8. Margaret M. Fleck. Perspective projection: The wrong imaging model. Research report 95-01, Department of Computer Science, University of Iowa, Iowa City, USA, 1995.

9. Joshua Gluckman and Shree K. Nayar. Ego-motion and omnidirectional cameras. In Sharat Chandran and Uday Desai, editors, *The Sixth International Conference on Computer Vision in Bombay, India*, pages 999–1005, 6 Community Centre, Panscheel Park, New Delhi 110 017, January 1998. N. K. Mehra for Narosa Publishing House.
10. Francis Hamit. New video and still cameras provide a global roaming viewpoint. *Advance Imaging*, pages 50–52, March 1997.
11. Richard I. Hartley. Euclidean reconstruction from uncalibrated views. In *Workshop on Invariants in Computer Vision*, pages 187 – 202, October 1993.
12. Richard I. Hartley. In defence of the 8-point algorithm. In *Fifth International Conference on Computer Vision, MIT Cambridge Massachusetts*, pages 1064–1070. IEEE Copmuter Society Press, 1995.
13. Hiroshi Ishiguro, Masashi Yamamoto, and Saburo Tsuji. Omni–directional stereo. *IEEE Transactions on Pattern Analysis and Machine Inteligence*, 14(2):257–262, February 1992.
14. Shree K. Nayar. Catadioptric omnidirectional camera. In *International Conference on Computer Vision and Pattern Recognition 1997, Puerto Rico USA*, pages 482–488. IEEE Computer Society Press, June 1997.
15. Sameer A. Nene and Shree K. Nayar. Stereo with mirrors. In Sharat Chandran and Uday Desai, editors, *The Sixth International Conference on Computer Vision in Bombay, India*, pages 1087–1094, 6 Community Centre, Panscheel Park, New Delhi 110 017, January 1998. N. K. Mehra for Narosa Publishing House.
16. Tomáš Pajdla. BCRF - Binary Illumination Coded Range Finder: Reimplementation. ESAT MI2 Technical Report Nr. KUL/ESAT/MI2/9502, Katholieke Universiteit Leuven, Belgium, April 1995.
17. David Southwell, Anup Basu, Mark Fiala, and Jereome Reyda. Panoramic stereo. In *International Conference on Pattern Recognition 1996, Vienna, Austria*, volume A, pages 378–382. IEEE Computer Society Press, August 1996.
18. Tomáš Svoboda, Tomáš Pajdla, and Václav Hlaváč. Central panoramic cameras: Geometry and design. Research report K335/97/147, Czech Technical University, Faculty of Electrical Engineering, Center for Machine Perception, December 1997. Available at ftp://cmp.felk.cvut.cz/pub/cmp/articles/svoboda/TR-K335-97-147.ps.gz.
19. Yasushi Yagi, Yoshimitsu Nishizawa, and Masahiko Yachida. Map-based navigation for a mobile robot with omnidirectional images sensor COPIS. *IEEE Transaction on Robotics and Automation*, 11(5):634–648, October 1995.
20. Yasushi Yagi, Kazuma Yamazawa, and Masahiko Yachida. Rolling motion estimation for mobile robot by using omnidirectional image sensor hyperomnivision. In *International Conference on Pattern Recognition 1996, Vienna, Austria*, pages 946–950. IEEE Computer Society Press, September 1996.
21. Zhengyou Zhang, Rachid Deriche, Olivier Faugeras, and Quang-Tuang Luog. A robust technique for matching two uncalibrated images through the recovery of the unknown epipolar geometry. *Artificial Inteligence*, 78:87–119, October 1995. Also Research Report No.2273, INRIA Sophia-Antipolis.